

Compton scattering, meson exchange, and the polarizabilities of bound nucleons

G. Feldman,¹ K. E. Mellendorf,² R. A. Eisenstein,^{2,*} F. J. Federspiel,^{2,†} G. Garino,^{2,‡} R. Igarashi,¹ N. R. Kolb,¹ M. A. Lucas,^{2,§} B. E. MacGibbon,² W. K. Mize,² A. M. Nathan,² R. E. Pywell,¹ and D. P. Wells^{2,||}
¹Saskatchewan Accelerator Laboratory, University of Saskatchewan, Saskatoon, Saskatchewan, Canada S7N 5C6
²Department of Physics, University of Illinois at Urbana-Champaign, Urbana, Illinois 61801

(Received 6 June 1996)

Elastic photon scattering cross sections on ^{16}O have been measured in the energy range 27–108 MeV. These data are inconsistent with a conventional interpretation in which the electric and magnetic polarizabilities of the bound nucleon are unchanged from the free values and the meson-exchange seagull amplitude is taken in the zero-energy limit. Agreement with the data can be achieved by invoking either strongly modified polarizabilities or a substantial energy dependence to the meson-exchange seagull amplitude. It is argued that these seemingly different explanations are experimentally indistinguishable and probably physically equivalent. [S0556-2813(96)50911-8]

PACS number(s): 13.60.Fz, 14.20.Dh, 21.30.Fe, 25.20.Dc

The electric and magnetic polarizabilities, labeled $\bar{\alpha}$ and $\bar{\beta}$, respectively, measure the ease with which a static external electric or magnetic field can induce an electric or magnetic dipole moment in a composite system. The nucleon itself is a composite system, and its polarizabilities constitute fundamental structure constants that are as important as the charge and magnetic radii. In recent years, a series of measurements has yielded reasonably precise values for both the proton [1–4] and neutron [5]:

$$\begin{aligned}\bar{\alpha}_p &= 12.1 \pm 0.8 \pm 0.5, & \bar{\beta}_p &= 2.1 \mp 0.8 \mp 0.5, \\ \bar{\alpha}_n &= 12.6 \pm 1.5 \pm 2.0, & \bar{\beta}_n &= 3.2 \mp 1.5 \mp 2.0.\end{aligned}\quad (1)$$

Above and hereafter all polarizabilities are quoted in units of 10^{-4} fm^3 . For the proton, the first error is the combined statistical and systematic uncertainty based on the results of several experiments, and the second error represents an estimated theoretical uncertainty based on the model dependence in the extraction of the polarizabilities from the Compton scattering cross sections [4]. For the neutron, the first error is statistical and the second error is systematic.

Along with the experimental activity, there has been considerable theoretical progress. Although there are still quantitative questions that remain unanswered, a picture is starting to emerge in which valence quarks and virtual pions both play an important role. It now appears that valence quarks contribute very little to either $\bar{\alpha}$ or the diamagnetic (or negative) part of $\bar{\beta}$, and instead these quantities are dominated by

the pion cloud [6–9]. In effect, the presence of an external electromagnetic field polarizes the pion cloud and, to the extent that the pions are polarizable, will polarize the pions themselves [10–12]. On the other hand, the paramagnetic (or positive) part of $\bar{\beta}$ is due almost entirely to the Δ resonance [13], which is largely a valence quark excitation. Cancellation between the paramagnetic and diamagnetic parts gives rise to a low value of $\bar{\beta}$.

The important role played by the pion cloud raises the question of whether the polarizabilities of a nucleon are modified in the nuclear medium. Since the pion cloud extends well into the periphery of the nucleon, it is not unreasonable to expect it to be distorted by the presence of nearby nucleons, thereby resulting in a modification of the polarizabilities, as suggested by Ericson and Rosa-Clot [14] and by Bunatyan [15]. Experimental results thus far remain inconclusive on this issue. In these experiments, angular distributions of the Compton scattering cross section from nuclear targets are measured, and the polarizabilities of the bound nucleon are deduced with the aid of a semi-phenomenological formalism [16–19], which is discussed more fully below. Recent work by a Lund/Göttingen collaboration [19] indicates no modification of the free polarizabilities in ^{12}C and ^{16}O ; however, the same group [20] finds a substantial modification in ^4He , $\Delta\bar{\beta} = -\Delta\bar{\alpha} \approx 7$.

In this paper, we report new and more extensive measurements of the Compton scattering cross section on ^{16}O . When interpreted in the context of the same formalism, these data unambiguously establish a strong modification of the bound nucleon polarizabilities from the free values or, alternately, a substantial deviation of the meson-exchange seagull amplitude from the low-energy limit. This result is in qualitative agreement with the recent calculation of Hütt and Milstein [21], as discussed below.

Photon scattering cross sections were measured over the energy range 27–108 MeV in two separate but nearly identical experiments using the tagged photon facilities at the University of Illinois [22] and the Saskatchewan Accelerator Laboratory (SAL) [23]. In both experiments, high duty-factor beams of electrons were incident on a thin aluminum radiator. The resulting bremsstrahlung photons were colli-

*Present address: Physics Division, National Science Foundation, Arlington, VA 22230.

†Present address: MP-4, LANL, MS H846, Los Alamos, NM 87545.

‡Present address: Institute for Nuclear Study, University of Tokyo, Tokyo 188, Japan.

§Present address: Brookhaven National Laboratory, Upton, NY 11973.

||Present address: Department of Physics, Idaho State University, Pocatello, ID 83209.

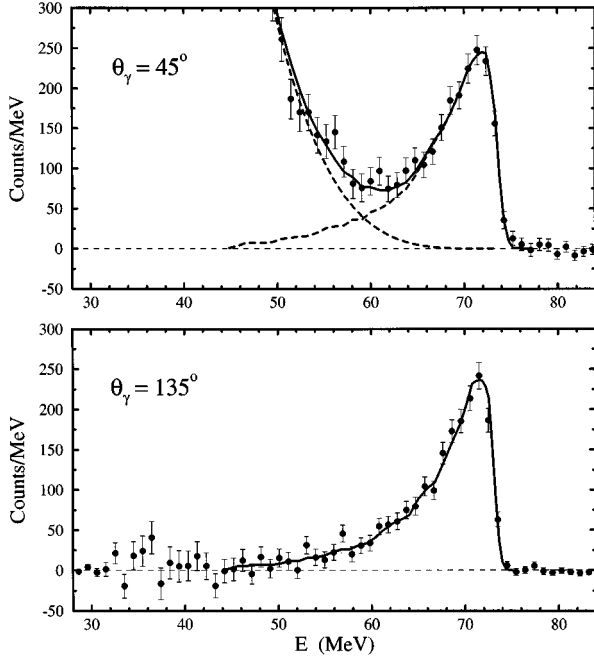


FIG. 1. Spectra of photons scattered from ^{16}O at an incident photon energy of 74 MeV. The curves are fits to the data using line shapes generated by a Monte Carlo code and including a smooth background for the 45° spectrum.

mated, scattered from a water target, and detected in coincidence with the momentum-analyzed residual electrons, thereby tagging the incident photon. This in turn permitted an accurate measurement of the incident photon flux by simply counting the associated tagging electrons, which were detected in a multi-element hodoscope of plastic scintillators. By periodically placing one of the photon detectors directly in the photon beam, the number of tagged photons per tagging electron was determined and was constant throughout the course of each experiment to within a few percent. An important feature of this technique is that the same detectors are used to calibrate the incident flux as are used to count the scattered photons. Thus, to lowest order, the absolute normalization does not depend on the efficiency or line-shape response of the photon detector. Corrections to the normalization for these effects, which were calculated using a Monte Carlo simulation [22] based on electromagnetic shower codes [24], typically were less than about 5%.

The scattering target of distilled water was contained in a thin-walled Lucite box, 7.6 cm thick, with 0.13 mm Mylar entrance and exit windows for the incident beam. The photon detectors were two large cylindrical NaI(Tl) crystals placed at 45° and 135° with respect to the photon beam axis. For the energy range 89–108 MeV, data were also taken with the detectors at 90° . Each detector subtended a solid angle of about 0.05 sr and was surrounded by both passive and active shielding. The Illinois experiment covered the tagged photon energy range 27–64 MeV in five separate data runs, each subdivided into 32 contiguous energy bins. The SAL experiment covered the range 60–108 MeV in two separate data runs, each subdivided into 62 energy bins.

In order to extract the number of scattered photons from the spectrum, a peak-fitting procedure was utilized, with line

shapes calculated from the Monte Carlo code. For the 45° data, a smooth background was included in the fitted shape to account for atomic processes. Typical spectra of coincidence events, corrected for accidental coincidences, and the corresponding fits are shown in Fig. 1.

The cross sections, suitably averaged over tagging bins, are shown in Fig. 2, along with the Lund/Göttingen data [19]. The latter cross sections are significantly lower than the present ones at the backward angle. The overall systematic uncertainty in the absolute cross sections is approximately $\pm 5\%$. Further details about the experimental setup and procedures, data reduction, and systematic errors can be found in Ref. [22].

In order to interpret the scattering cross sections, the complex scattering amplitude is written as [16–19]

$$R(E, \theta) = R^{GR}(E, \theta) + R^{QD}(E, \theta) + R_1^{SG}(E, \theta) + R_2^{SG}(E, \theta), \quad (2)$$

where E and θ are the laboratory photon energy and scattering angle, respectively. The four terms refer to the giant resonance (GR), the quasideuteron (QD), and the one- and two-body seagull (SG) amplitudes, respectively. The GR and QD amplitudes are expanded as follows:

$$R^{GR}(E, \theta) = f_{E1}(E)g_{E1}(\theta) + f_{E2}(E)g_{E2}(\theta) + \frac{NZ}{A}r_0[1 + \kappa_{GR}]g_{E1}(\theta), \quad (3)$$

and

$$R^{QD}(E, \theta) = \left[f_{QD}(E) + \frac{NZ}{A}r_0\kappa_{QD} \right] F_2(q)g_{E1}(\theta), \quad (4)$$

where f_{E1} , f_{E2} , and f_{QD} are the forward scattering amplitudes due to the giant dipole resonance, the giant quadrupole resonance, and the quasideuteron process, respectively. These amplitudes are *uniquely determined* from the corresponding part of the total photoabsorption cross section via the optical theorem and a dispersion relation (cf. Eq. 8 of Ref. [17]). The factors $1 + \kappa_{GR}$ and κ_{QD} are the integrals of the GR and QD photoabsorption cross sections, respectively, in units of the classical dipole sum rule, and r_0 is the classical radius of the nucleon. The QD amplitude, being a manifestly two-body process, is modulated by a phenomenological two-body form factor $F_2(q)$, where q is the momentum transfer. The angular factors $g_\lambda(\theta)$ are known functions of the wave vector and polarization of the incident and scattered photon (cf. Table IV of Ref. [17]).

The seagull amplitudes take into account subnucleon and meson-exchange degrees of freedom that are not included in the GR and QD amplitudes, and they are required to preserve the gauge invariance of the full scattering amplitude. For energies sufficiently below the pion threshold, the one-body seagull is given by [18]

$$R_1^{SG}(E, \theta) = -F_1(q) \left\{ \left[Zr_0 - \left(\frac{E}{\hbar c} \right)^2 A \bar{\alpha} \right] g_{E1}(\theta) - \left[\left(\frac{E}{\hbar c} \right)^2 A \bar{\beta} \right] g_{M1}(\theta) + \mathcal{O}(E^4) \right\}, \quad (5)$$

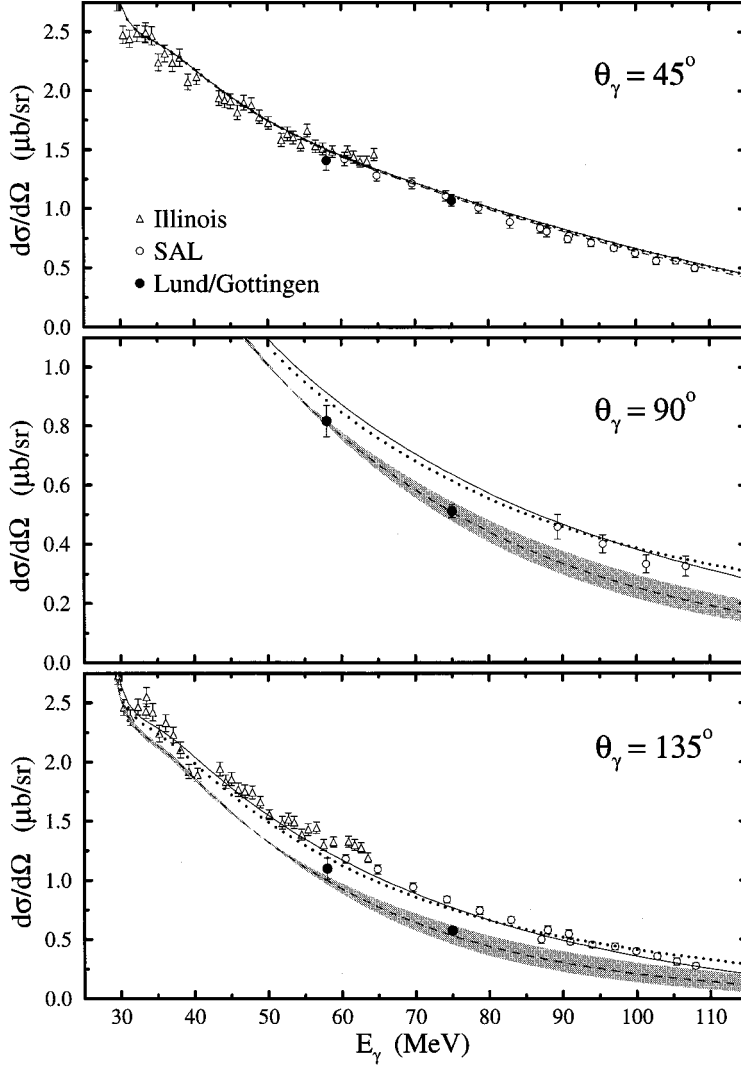


FIG. 2. Scattering cross sections at 45° , 90° , and 135° . The closed circle in the 135° plot at 75 MeV is actually an interpolation between the measured points at 127° and 150° in Ref. [19]. The dashed curve is the cross section calculated assuming the free nucleon polarizabilities and the low-energy limit of the exchange seagull amplitude. The shaded bands show the range of cross sections calculated under these assumptions as the $E2$ strength and the shape of the exchange form factor are varied. The solid and dotted curves utilize modified nucleon polarizabilities or modified exchange seagull, respectively, as discussed in the text. The good agreement of all three curves with the 45° data is expected since each curve obeys the sum-rule constraint, Eq. (7).

and the two-body seagull by [21,25–27]

$$R_2^{SG}(E, \theta) = -F_2(q) \left\{ \left[\frac{NZ}{A} \kappa r_0 - \left(\frac{E}{\hbar c} \right)^2 A \bar{\alpha}_{\text{ex}} \right] g_{E1}(\theta) - \left[\left(\frac{E}{\hbar c} \right)^2 A \bar{\beta}_{\text{ex}} \right] g_{M1}(\theta) + \mathcal{O}(E^4) \right\}, \quad (6)$$

where $\kappa = \kappa_{GR} + \kappa_{QD}$. Equation (5) is essentially the impulse approximation amplitude. It is the sum over all nucleons of the fundamental scattering amplitude from protons and neutrons,¹ expanded in powers of E^2 . The finite size of the nucleus gives rise to the modulation of this amplitude by the one-body form factor $F_1(q)$. The $\mathcal{O}(E^0)$ term in braces is the scattering amplitude from point protons. The $\mathcal{O}(E^2)$ terms involve $\bar{\alpha}$ and $\bar{\beta}$, which are identified as the average electric and magnetic polarizabilities of a bound nucleon [18] and are the parameters of primary interest in the present analysis. Equation (6) is the scattering amplitude from pairs of nucleons, commonly referred to as the exchange two-

photon amplitude [25]. The $\mathcal{O}(E^0)$ term in braces is completely constrained by a low-energy theorem, which requires the full amplitude at $E=0$ to be the classical Thomson amplitude for scattering from the total nuclear charge and mass [25,27]. The amplitude is modulated by the two-body form factor $F_2(q)$ [27,21]. Following Hütt and Milstein [21] and in analogy with the one-body seagull, the $\mathcal{O}(E^2)$ terms are modifications to the leading term, with parameters $\bar{\alpha}_{\text{ex}}$ and $\bar{\beta}_{\text{ex}}$ that formally look just like polarizabilities and about which little is known. In the conventional analysis [16,17], including that of Ref. [19], $\bar{\alpha}_{\text{ex}}$ and $\bar{\beta}_{\text{ex}}$ are set to zero, i.e., these and higher-order terms are ignored. In the present analysis, $\bar{\alpha}_{\text{ex}}$ and $\bar{\beta}_{\text{ex}}$ are treated as phenomenological parameters.

A forward dispersion relation leads to a model-independent sum rule:

$$(\bar{\alpha} + \bar{\beta}) + (\bar{\alpha}_{\text{ex}} + \bar{\beta}_{\text{ex}}) = \frac{\hbar c}{2\pi^2 A} \int_{m_\pi c^2}^{\infty} \frac{\sigma_T(E) - \sigma_{QD}(E)}{E^2} dE \approx 15, \quad (7)$$

¹Since ^{16}O is a spin-saturated nucleus, only the spin-averaged amplitude is required.

where σ_T and σ_{QD} are the total and QD photoabsorption

cross sections, respectively.² The numerical value, which comes from evaluation of the integral using a combination of experimental data and systematics [30,31], is very close to the value for the free nucleon, suggesting that $\bar{\alpha}_{\text{ex}} + \bar{\beta}_{\text{ex}} \approx 0$. There is no similarly straightforward sum rule for other combinations of the polarizabilities [32,12], so that the seagull amplitude represents new physics obtained from Compton scattering that is not already constrained by the photoabsorption cross section. Moreover, since the scattering cross section is sensitive primarily to $(\bar{\alpha} \pm \bar{\beta}) + (\bar{\alpha}_{\text{ex}} \pm \bar{\beta}_{\text{ex}})$ at forward and backward angles, respectively, the new physics is manifested primarily at backward angles. Finally, the structure of Eqs. (5) and (6) shows that it is not easily possible to separately determine the one-body and two-body polarizabilities, since they enter coherently into the scattering amplitude with the same energy dependence and only a slightly different form factor.

The operational aspects of the formalism can be summarized as follows. For a given $\sigma_T(E)$, including its decomposition into $E1$, $E2$, and QD parts, the f_λ in Eqs. (3) and (4) as well as κ_{GR} and κ_{QD} are calculated. The one-body form factor is taken to be that measured in elastic electron scattering [29], and the exchange form factor is initially taken to be that expected for two uncorrelated nucleons: $F_2(q) = [F_1(q/2)]^2$. The latter implies a mean-square exchange radius $\langle r_{\text{ex}}^2 \rangle$ exactly half of the mean-square charge radius $\langle r^2 \rangle$. The only unknowns are the four polarizabilities, subject to the sum-rule constraint [Eq. (7)]. In practice, σ_T is parametrized as a sum of Lorentzian resonances plus a smooth QD curve. The parameters of σ_T are adjusted to fit simultaneously the 45° scattering cross sections (including those of Ref. [28]) and the experimental values for σ_T [31]. The $E2$ part of the cross section is fixed to be a narrow isoscalar resonance centered at 16 MeV and a broad isovector resonance centered at 60 MeV, each exhausting their respective energy-weighted sum rule (EWSR). The Compton scattering data themselves rule out narrow concentrations of $E2$ strength in the 30–100 MeV energy range [22]. With σ_T thus determined, and for a particular choice of polarizabilities, the backward-angle scattering cross sections can be compared with the data.

A summary of our essential results is given by the comparison between the curves and the data in Fig. 2. The dashed curve, which represents the cross section calculated in the conventional approach (i.e., using the free nucleon polarizabilities and no exchange polarizabilities), is not in agreement with the present 135° and 90° data, although it does accurately describe the data of Ref. [19]. The calculation can be brought into substantial agreement with the data by making $\Delta\bar{\beta} = -\Delta\bar{\alpha} \approx 8$ and $\bar{\beta}_{\text{ex}} = -\bar{\alpha}_{\text{ex}} = 0$ (solid curve)

²In the present formalism, f_{QD} in Eq. (4) is obtained from σ_{QD} via a dispersion integral whose upper limit is infinity. In order not to double count, we subtract σ_{QD} from σ_T in the sum rule. Alternately one could terminate the dispersion integral for f_{QD} at $m_\pi c^2$ and not subtract σ_{QD} in Eq. (7), thereby redefining the meaning of the polarizabilities. Our approach reflects the point of view, shared by the authors of Ref. [19], that the nucleon polarizabilities are associated only with *nucleon* excitations.

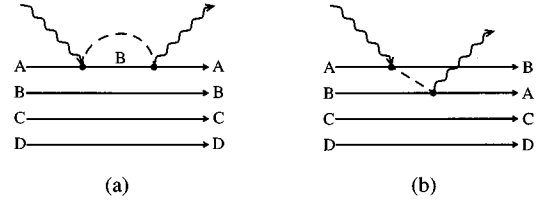


FIG. 3. (a) Diagram giving rise to a reduction in $\bar{\alpha}$ due to Pauli blocking. (b) Corresponding exchange diagram, which leads to a negative $\bar{\alpha}_{\text{ex}}$.

or $\Delta\bar{\beta} = -\Delta\bar{\alpha} = 0$ and $\bar{\beta}_{\text{ex}} = -\bar{\alpha}_{\text{ex}} \approx 5$ (dotted curve), where Δ refers to the change relative to the free value. The size of the discrepancy between the dashed curve and the data (and therefore the size of the modified polarizabilities) depends in detail on the magnitude and distribution of $E2$ strength and on the shape of the exchange form factor. This is demonstrated by the shaded bands in Fig. 2, which show the range of calculated cross sections, assuming unmodified polarizabilities, as the $E2$ strength and shape of $F_2(q)$ are varied. Specifically, the bands represent the effect of varying the integrated isovector $E2$ strength in the range $(0.5 - 1.5)\text{EWSR}$ and $\langle r_{\text{ex}}^2 \rangle$ in the range $(0.33 - 0.66)\langle r^2 \rangle$. Modified polarizabilities in the range $\Delta\bar{\beta} = -\Delta\bar{\alpha} \approx 5 - 11$ are needed to bring these calculations into agreement with experiment. These uncertainties preclude a precise measurement of $\Delta\bar{\beta}$. Nevertheless, any reasonable choice of $E2$ strength or exchange form factor leads to the same conclusion: either a substantial modification of the nucleon polarizabilities or a significant energy dependence to the exchange seagull amplitude is required. This is the principal result from this work. This conclusion is consistent with the earlier work of Fuhrberg *et al.* in ^4He [20] but contrasts with that of Häger *et al.* in ^{12}C and ^{16}O [19]. The different conclusion reached by Häger *et al.* is due entirely to the disagreement in cross sections.

The curves in Fig. 2 emphasize that a modification to the free nucleon polarizabilities is nearly indistinguishable from an energy dependence to the exchange seagull amplitude. It can be argued that these are two equivalent descriptions of the same physics. We focus the discussion only on $\bar{\alpha}$, which arises in lowest-order chiral perturbation theory [7] from diagrams involving a single pion loop (i.e., scattering from the virtual pion cloud). In nuclei, some of these diagrams are Pauli blocked, as shown in Fig. 3(a), resulting in a reduction in $\bar{\alpha}$. However, as pointed out by Drell and Walecka [33], the blocked diagrams may be included, thereby restoring $\bar{\alpha}$ to its free value, provided the corresponding exchange diagrams of Fig. 3(b) are also included, thereby giving rise to a nonzero $\bar{\alpha}_{\text{ex}}$. Since the blocked diagrams are *exactly* the negative of the corresponding exchange diagrams,³ a reduction in $\bar{\alpha}$ is equivalent to a negative $\bar{\alpha}_{\text{ex}}$. Hütt and Milstein [21] have calculated $\bar{\beta}_{\text{ex}}$ and $\bar{\alpha}_{\text{ex}}$ for symmetric nuclear matter using a nonrelativistic Fermi gas model. They find

³Because of the antisymmetry of the nuclear wave function, the exchange amplitude introduces a negative sign when states A and B are interchanged. See Fig. 1 of Ref. [33].

$\bar{\beta}_{\text{ex}} \approx +1.7$ and $\bar{\alpha}_{\text{ex}} \approx -3.2$, in qualitative agreement with our experimental result.

In summary, we have measured an extensive set of Compton scattering cross sections on ^{16}O using tagged photons in the energy range 27–108 MeV. Calculations employing giant resonance, quasideuteron, and one- and two-body seagull amplitudes have been shown to reproduce the data only if (1) a substantial modification to the nucleon polarizability is introduced, or (2) an energy-dependent term is included in the meson-exchange seagull amplitude. These two variations

have been demonstrated to be nearly indistinguishable experimentally and are probably physically equivalent.

We thank Dr. A. Milstein for allowing us to refer to the calculations of Ref. [21] prior to publication. We acknowledge fruitful discussions with Dr. A. L'vov and thank Dr. J. Friar for pointing out the argument in Ref. [33]. This research was supported in part by the Natural Sciences and Engineering Research Council of Canada and by the U.S. National Science Foundation under Grant Nos. NSF PHY 89-21146, 93-10871, and 94-20787.

-
- [1] F. J. Federspiel, R. A. Eisenstein, M. A. Lucas, B. E. MacGibbon, K. Mellendorf, A. M. Nathan, A. O'Neill, and D. P. Wells, *Phys. Rev. Lett.* **67**, 1511 (1991).
- [2] A. Zieger, R. Van de Vyver, D. Christmann, A. De Graeve, C. Van den Abeele, and B. Ziegler, *Phys. Lett. B* **278**, 34 (1992).
- [3] E. L. Hallin *et al.*, *Phys. Rev. C* **48**, 1497 (1993).
- [4] B. E. MacGibbon, G. Garino, M. A. Lucas, A. M. Nathan, G. Feldman, and B. Dolbilkin, *Phys. Rev. C* **52**, 2097 (1995).
- [5] J. Schmiedmayer, P. Riehs, J. A. Harvey, and N. W. Hill, *Phys. Rev. Lett.* **66**, 1015 (1991).
- [6] R. Weiner and W. Weise, *Phys. Lett.* **159B**, 85 (1985).
- [7] V. Bernard, N. Kaiser, and U.-G. Meissner, *Phys. Rev. Lett.* **66**, 1515 (1991).
- [8] B. R. Holstein, *Comments Nucl. Part. Phys.* **20**, 201 (1992).
- [9] A. I. L'vov, *Phys. Lett. B* **304**, 29 (1993).
- [10] V. M. Budnev and V. A. Karnakov, *Yad. Fiz.* **30**, 440 (1979) [*Sov. J. Nucl. Phys.* **30**, 228 (1979)].
- [11] W. Broniowski and T. S. Cohen, *Phys. Rev. D* **47**, 299 (1993).
- [12] B. R. Holstein and A. M. Nathan, *Phys. Rev. D* **49**, 6101 (1994).
- [13] N. C. Mukhopadhyay, A. M. Nathan, and L. Zhang, *Phys. Rev. D* **47**, R7 (1993).
- [14] M. Ericson and M. Rosa-Clot, *Phys. Lett. B* **188**, 11 (1987); *Z. Phys. A* **324**, 373 (1986); *Z. Phys. A* **320**, 675 (1985); *Nuovo Cimento* **76A**, 180 (1983).
- [15] G. G. Bunatyan, *Yad. Fiz.* **55**, 3196 (1992) [*Sov. J. Nucl. Phys.* **55**, 1781 (1992)].
- [16] M. Schumacher, P. Rullhusen, and A. Baumann, *Nuovo Cimento* **100A**, 339 (1988).
- [17] D. H. Wright, P. T. Debevec, L. J. Morford, and A. M. Nathan, *Phys. Rev. C* **32**, 1174 (1985).
- [18] D. Drechsel and A. Russo, *Phys. Lett.* **137B**, 294 (1984).
- [19] D. Häger *et al.*, *Nucl. Phys.* **A595**, 287 (1995); M. Ludwig *et al.*, *Phys. Lett. B* **274**, 275 (1992).
- [20] K. Fuhrberg *et al.*, *Nucl. Phys.* **A591**, 1 (1995).
- [21] M.-Th. Hütt and A. I. Milstein, *Nucl. Phys. A* (to be published).
- [22] K. E. Mellendorf, Ph.D. thesis, University of Illinois, 1993 (University Microfilms International).
- [23] J. M. Vogt, R. E. Pywell, D. M. Skopik, E. L. Hallin, J. C. Bergstrom, H. S. Caplan, K. I. Blomqvist, W. Del Bianco, and J. W. Jury, *Nucl. Instrum. Methods Phys. Res. A* **324**, 198 (1993).
- [24] W. R. Nelson *et al.*, Report No. SLAC-265, 1985 (unpublished); R. Brun *et al.*, GEANT 3.14, CERN 1990 (unpublished).
- [25] H. Arenhövel, *Z. Phys. A* **297**, 129 (1980); M. Weyrauch and H. Arenhövel, *Nucl. Phys.* **A408**, 425 (1983).
- [26] J. L. Friar, *Ann. Phys. (N.Y.)* **95**, 170 (1975); J. L. Friar, *Phys. Rev. Lett.* **36**, 510 (1976).
- [27] W. M. Alberico and A. Molinari, *Z. Phys. A* **309**, 143 (1982).
- [28] S. F. LeBrun, S. D. Hoblit, and A. M. Nathan, *Phys. Rev. C* **35**, 2005 (1987).
- [29] C. W. deJager, H. deVries, and C. deVries, *At. Data Nucl. Data Tables* **14**, 479 (1979).
- [30] J. Ahrens, *Nucl. Phys.* **A446**, 229c (1985).
- [31] J. Ahrens *et al.*, *Nucl. Phys.* **A251**, 479 (1975), and private communication.
- [32] A. I. L'vov, V. A. Petrun'kin, and S. A. Startsev, *Yad. Fiz.* **29**, 1265 (1979) [*Sov. J. Nucl. Phys.* **29**, 651 (1979)].
- [33] S. D. Drell and J. D. Walecka, *Phys. Rev.* **120**, 1069 (1960).